An investigation of geomagnetic effects on modern submarine cables: power feed configuration, uncertainties, and frequency response

S. Chakraborty[1], D. H. Boteler[2], M. D. Hartinger[3], X. Shi[4], P. Lomas[5], J. B. H. Baker[6], M. Macalester[7]

(1) Embry-Riddle Aeronautical University, Daytona Beach, FL (2) Natural Resources Canada, (3) Space Science Institute, (4) Clemson University, (5) Australia Japan Cable Network (6) Virginia Tech (7) Cybersecurity and Infrastructure Security Agency

Motivation and Objective of the Study

Modern submarine cables form the backbone of global connectivity, yet their vulnerability to extreme geomagnetic disturbances remains insufficiently quantified. Induced geoelectric fields drive voltages into power-feed equipment (PFE), threatening repeater saturation and trans-oceanic communication services.

- ❑ The **Australia-Japan Cable (AJC)** runs ~12800 km across the Western Pacific, Sydney to Kitakyushu via Guam — a representative low latitude modern submarine system.
- ❑ AJC shore stations record the end-to-end **Power Feed Equipment (PFE)** voltage continuously, providing a rare ground-truth dataset.
- ❑ We plan to apply the **SCUBAS** (*Submarine Cable Upset By Auroral Streams*) physics-based GIC model to quantify the induced voltages along the submarine cables during May 10-11, 2024 'Gannon' superstorm (Dst_{min} ~ -412 nT) as a case study.
- ❑ Cable topology — route orientation, configuration, and water depth — strongly controls the spatial distribution and magnitude of induced voltages.

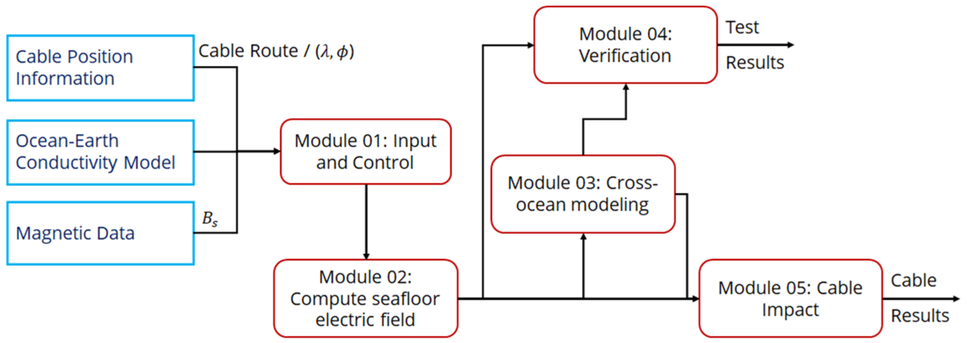

Figure 1 *– Control flow diagram of operations done by computational model. The boxes in red and blue define operational and input modules, respectively.*

- ➢Model can digest cable position, magnetic data, and ocean-earth conductivity model
- ➢Compute transfer function (T_x) that relates seafloor electric field (E_f) to surface magnetic field (B_s)
- ➢Compute E_f using T_x and B_s for each cable section.

Combine the effect of different cable sections to get total effect on cable.

Cable Geometry and Subsea Conductivity

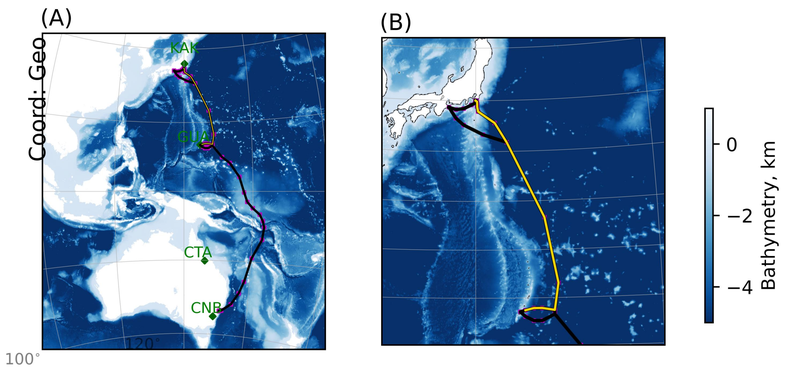

Figure 2 *– (A) AJC cable route overlaid on General Bathymetric Chart of the Oceans (GEBCO 2024) bathymetry. Key magnetometer stations (KAK, GUA, CNB, CTA) are marked in green. (B) Zoomed-in view of the Japan–Guam segment, showing route discretization and water depth, used in this study.*

We have implemented the SCUBAS pipeline for the Japan–Guam segment of the AJC, driven by KAK and GUA magnetometer data, and validated against observed PFE voltages at the terminal stations.

Data Sources

Dataset	Description
IAGA 2002	1-min X and Y components; KAK (Japan), GUA (Guam), CNB & CTA (Australia)
AJC PFE Recordings	Shore-station voltage at Tumon Bay (Guam) and Maruyama (Japan), from AJC operator
OMNI (1-min)	IMF/SW Conditions, AE, Sym-H, dynamic pressure
LITHO1.0	1-degree global lithospheric model; segment conductivity profiles, and water depth

Event Study and Results

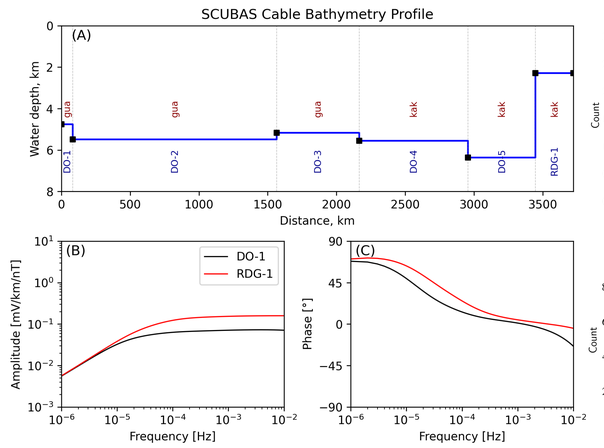

Figure 3 *– (A) Bathymetry depth profile of the Japan--Guam cable (~3700,km). Segments DO-1-to-DO-3 (3-7,km depth) are driven by GUA; DO-4,5 and ridge segment RDG-1 (~1.7,km, near Japan) is driven by KAK. (B,C) Transfer-function amplitude and phase for DO-1 (black) vs. RDG-1 (red): the shallower ridge exhibits ~0.5-1 decade higher amplitude at sub-mHz frequencies, demonstrating order-of-magnitude GIC sensitivity variation from bathymetry alone.*

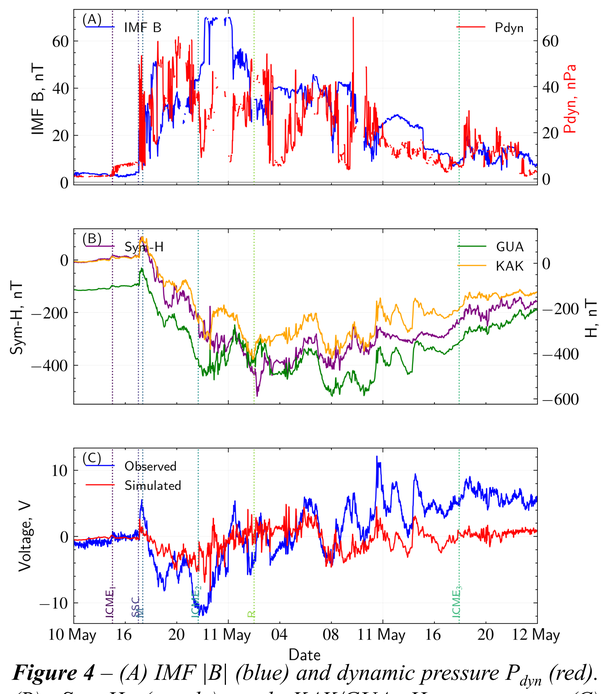

Figure 4 *– (A) IMF |B| (blue) and dynamic pressure P_{dyn} (red). (B) Sym-H (purple) and KAK/GUA H-components. (C) Observed AJC PFE voltage (blue) versus SCUBAS model (red); dashed vertical lines mark storm epochs. Both stations recorded extreme perturbations during the Gannon storm: |ΔH| at KAK exceeded 400 nT and |ΔH| at GUA exceeded 300 nT, providing strong broadband forcing across all cable segments simultaneously.*

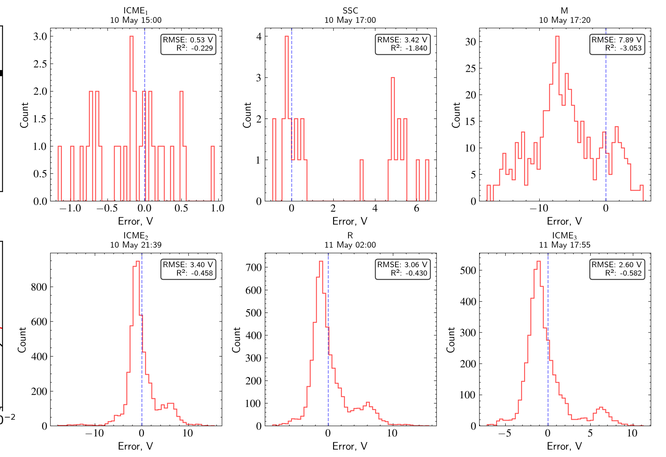

Figure 5 *– Error distribution histograms per storm phase (ICME₁, SSC, main, ICME₂, recovery, ICME₃). Each panel shows the residual (observed − modelled) distribution with RMSE and R^2 metrics. Negative R^2 indicates high signal variance relative to model amplitude. Errors are largest during the main phase and decrease as storm intensity diminishes.*

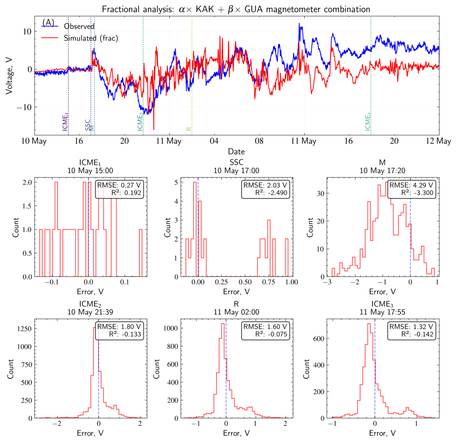

Figure 6 *– Fractional magnetometer analysis using α×KAK + β×GUA linear combination. (A) Time series comparing observed vs simulated voltage with storm phase markers. (B–G) Error distribution histograms per storm phase showing RMSE and R^2 metrics. Decreased RMSE and increased R^2 values compared to single-station forcing, indicating that combined magnetometer input better reproduces voltage measuements, however, this method introduces uncertainty due to spatial interpolation between stations which will be addressed in future study via response characteristics.*

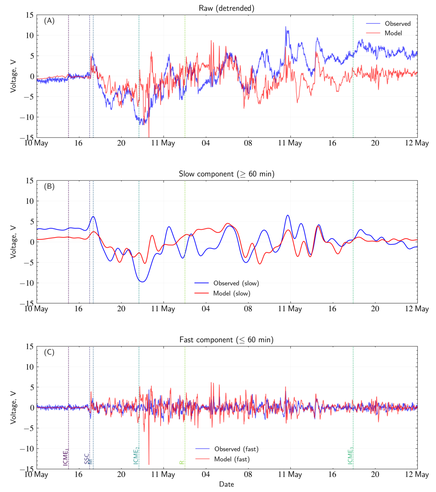

Figure 7 *– Detrended analysis separating temporal scales in the voltage signal. (A) Raw observed (blue) and modelled (red) voltage time series showing the full signal. (B) Slow component (>60 min periods) with linear trend removed, capturing storm-scale envelope variations. (C) Fast component (<60 min periods) revealing high-frequency sub-hourly fluctuations. This decomposition shows that the model captures the slow-varying storm envelope well, while high-frequency variations remain challenging to model accurately. Additionally, the model underestimates the slow-moving envelope but overestimates fast variations.*

Conclusions

- ➢SCUBAS captures the sign, onset, and slow temporal envelope of storm-induced voltages, but underestimates peak amplitude during intense main-phase periods.
- ➢Decreased RMSE and increased R^2 values compared to single-station forcing, indicating combined magnetometer input better constrains output; however, this method introduces uncertainty due to spatial interpolation between stations which will be addressed in future study via response characteristics.

Future work

1. Uncertainty Quantification: Quantify uncertainty in the calculated voltage / electric field.
2. Risk Assessment: How vulnerable are submarine cables during Carrington-type events or 1 in 100 or 1000 year events?

Acknowledgement

This work was supported by NSF GEM grant 2452540, and 2402336.

Refences